Electronic Supplementary Information (ESI)

of

Charge-Reversal Plug Gate Nanovalves on Peptide-Functionalized Mesoporous Silica Nanoparticles for Targeted Drug Delivery

Guo-Feng Luo, Wei-Hai Chen, Yun Liu, Jing Zhang, Si-Xue Cheng, Ren-Xi Zhuo and Xian-Zheng Zhang*

Key Laboratory of Biomedical Polymers of Ministry of Education & Department of Chemistry, Wuhan University, Wuhan 430072, P. R. China

Table S1. BET and BJH parameters of different nanoparticles.

Sample	BET surface area S_{BET} (m^2/g)	Pore volume V_p (cm^3/g)	BJH pore diameter W_{BJH} (Å)
MCM-41	1057.53	1.14	33.51
MSN-alkyne	802.50	0.89	31.92
MSN-K_8(Cit)	526.13	0.47	29.92
MSN-K_8(Cit)/K_8(RGD)$_2$	92.92	/	/

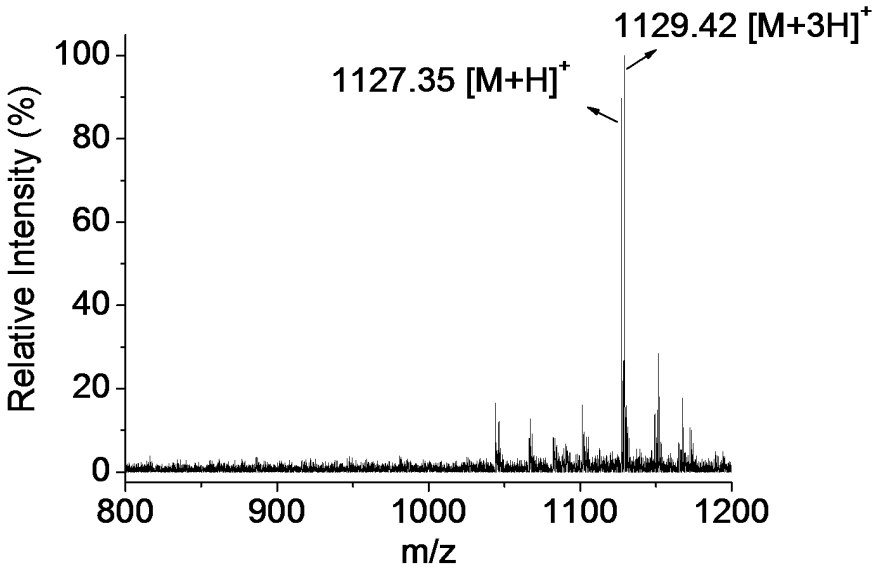

Fig. S1 MOLDI-TOF spectrum of K_8-azide.

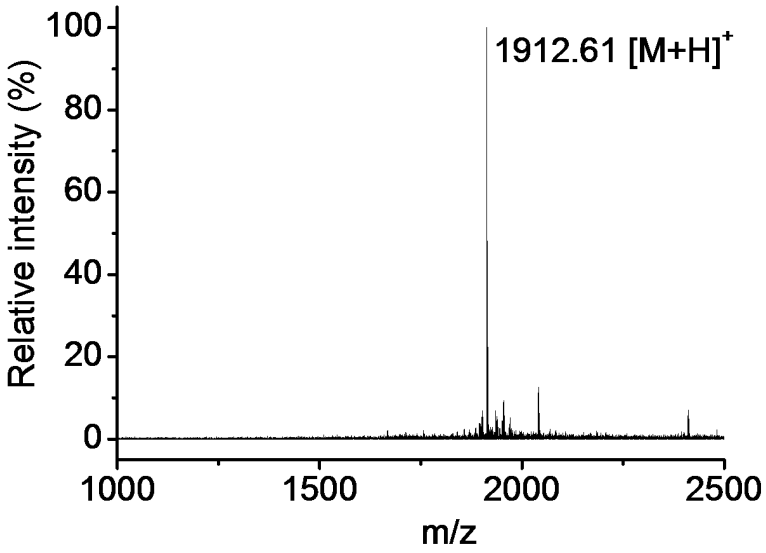

Fig. S2 MOLDI-TOF spectrum of $K_8(RGD)_2$.

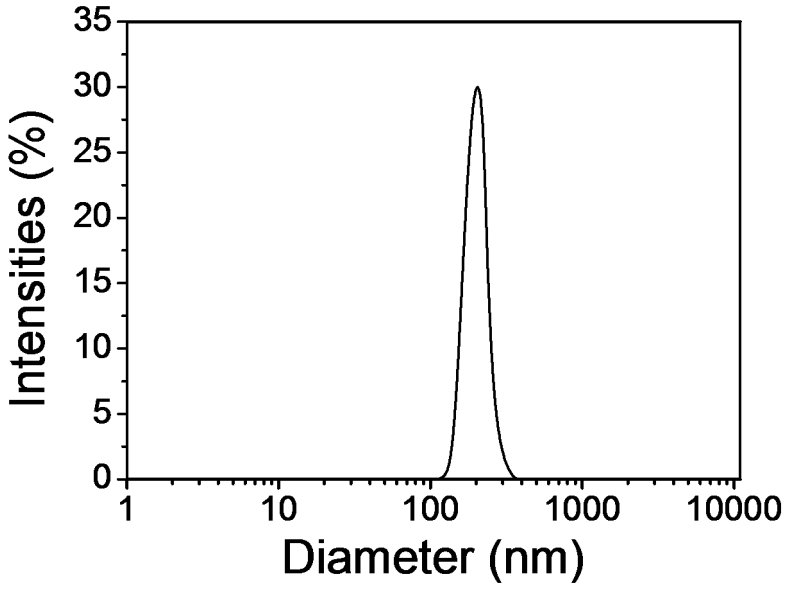

Fig. S3 Particle size and size distribution of MCM-41 in PBS (pH 7.4, 10 mM) at 37 ^{o}C.

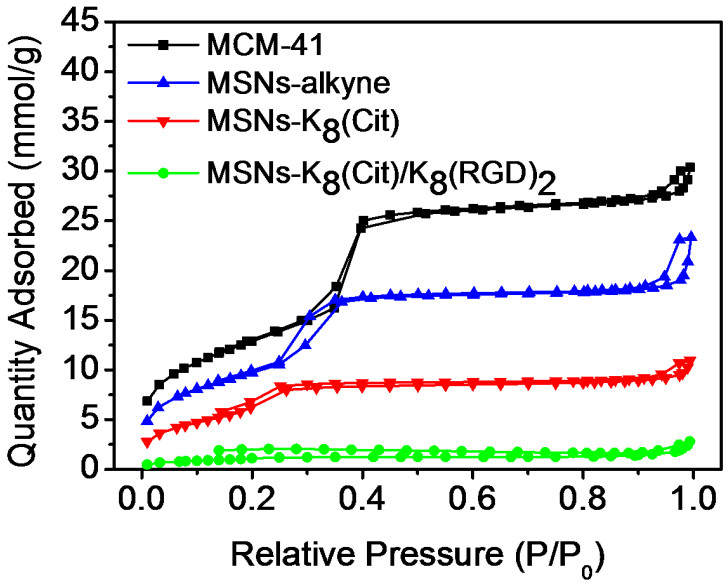

Fig. S4 Brunauer-Emmett-Teller (BET) nitrogen adsorption/desorption isotherms of MCM-41, MSN-alkyne, MSN-K_8(Cit), and MSN-K_8(Cit)/$K_8(RGD)_2$

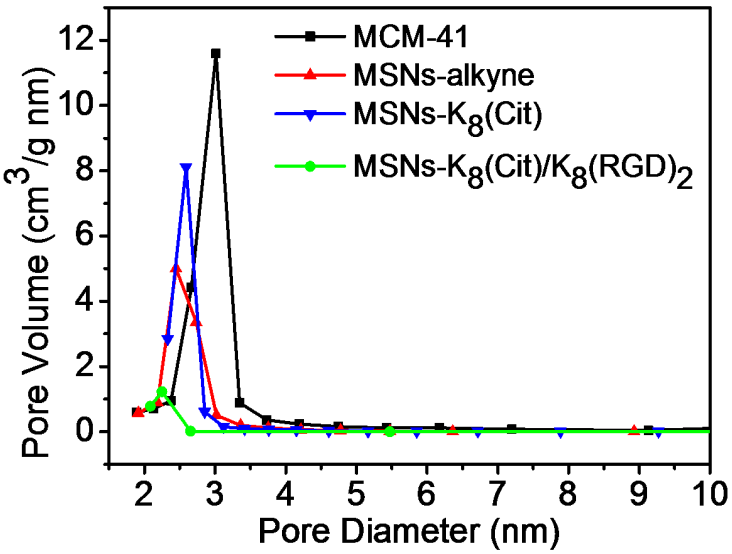

Fig. S5 Barrett-Joyner-Halenda (BJH) pore size distribution of MCM-41, MSN-alkyne, MSN-K_8(Cit), and MSN-K_8(Cit)/$K_8(RGD)_2$.

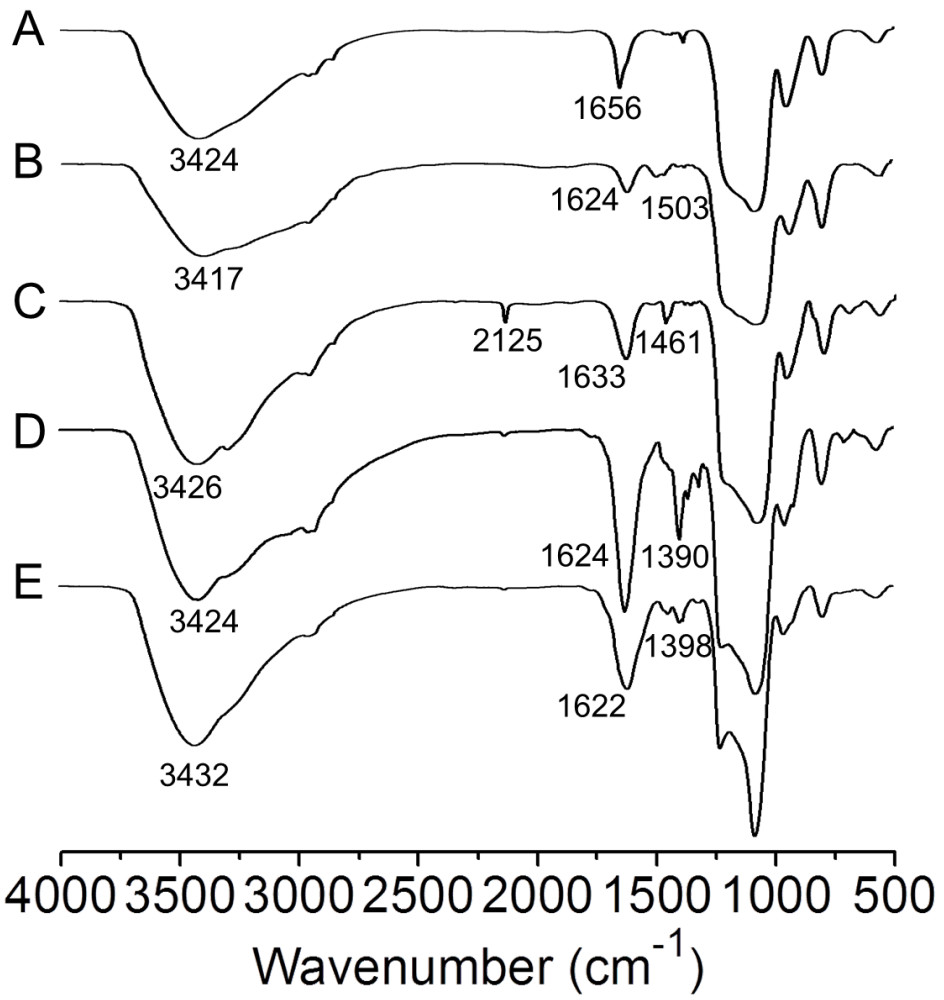

Fig. S6 FT-IR spectra of MCM-41(A), MSN-NH_2 (B), MSN-alkyne (C), MSN-K_8 (D), and MSN-K_8(Cit) (E).

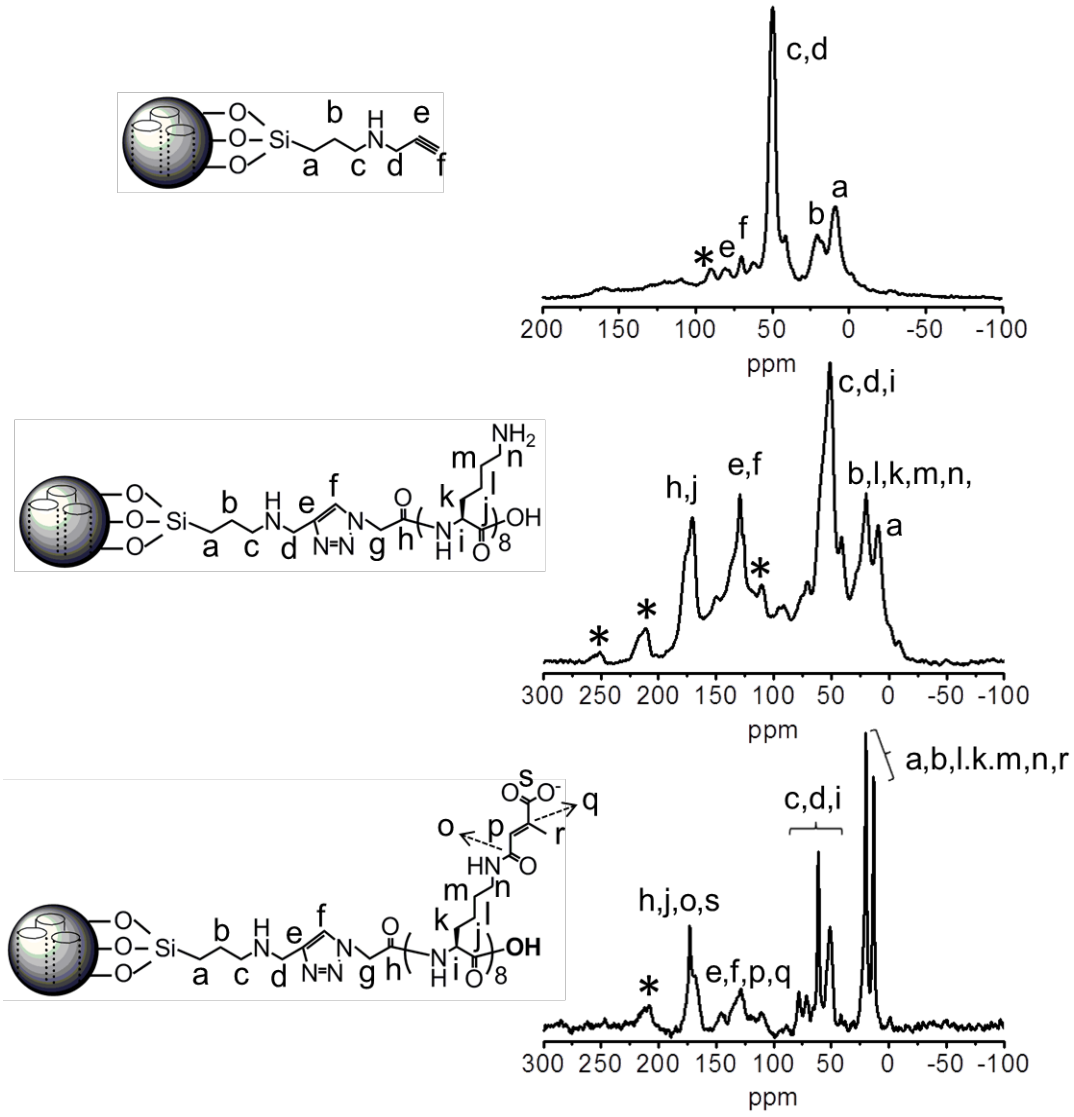

Fig. S7 ^{13}C CP/MAS NMR spectra of MSN-alkyne, MSN-K_8, and MSN-K_8(Cit). (* are spinning side bands)

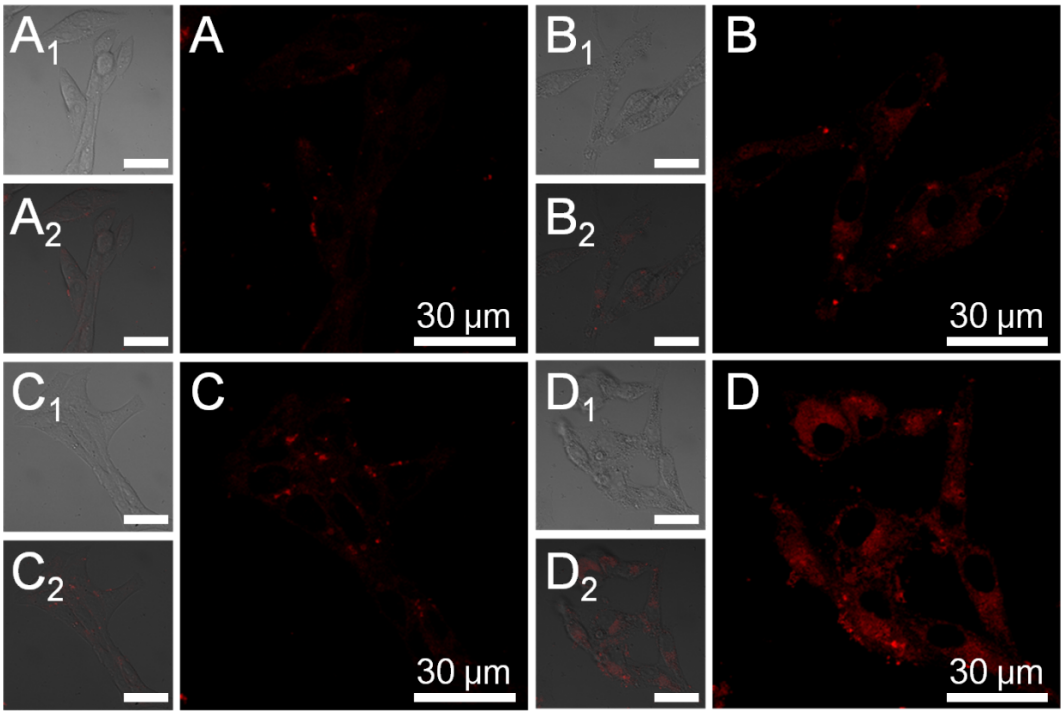

Fig. S8 CLSM images of COS7 (A, C) and U87 MG cells (B, D) treated by DOX@MSN-K_8(Cit)/K_8 (A, B) and DOX@MSN-K_8(Cit)/K_8(RGD)$_2$ (C,D) for 1 h.